11th International Symposium on Turbulence and Shear Flow Phenomena (TSFP11)
Southampton, UK, July 30 to August 2, 2019

VORTEX SHEDDING BEHIND AN INCLINED FLAT PLATE HINGED WITH A TRAILING-EDGE FLAP

Nonwarit Borvornsareepirom
Department of Mechanical Engineering
Chiang Mai University
Chiang Mai 50200, Thailand

Jiratrakul Tunkeaw
Department of Mechanical Engineering
Chiang Mai University
Chiang Mai 50200, Thailand

Watchapon Rojanaratanangkule*
Department of Mechanical Engineering
Chiang Mai University
Chiang Mai 50200, Thailand
*Correspondent author: watchapon.roj@eng.cmu.ac.th

ABSTRACT

An influence of a moving motion of a trailing-edge flap on the formation of the wake shed behind an inclined flat plate is investigated via the use of direct numerical simulation (DNS). The leading-edge plate is fixed at an angle of attack of 20°, while its rear part flaps according to a time-dependent equation. The chord based Reynolds number is 1000, while the freestream Mach number is set to 0.4. The movement of the trailing-edge flap alters the formation of the leading-edge and trailing-edge vortices. This leads to the modification of the evolution of the unsteady vortex shedding and the acoustic field, resulting in a reduction in the aerodynamic forces.

INTRODUCTION

The unsteady flow past bluff bodies has been investigated by several researches during the last several decades due to its immense applications in aviation. From the point of view of fluid mechanics, flow over a bluff body comprises several fluid flow phenomena, such as flow separation and vortex shedding. Lam & Wei (2010) studied the generation mechanism of the fluctuating lift and drag of an inclined flat plate and its relationship between the vortex shedding processes and the fluctuating aerodynamic force. The maximum lift occurs when the trailing-edge vortex sheds from the plate. On the other hand, the plate produces the minimum lift when the trailing-edge vortex is fully formed while still being attached to the plate. Yang *et al.* (2012) investigated the wake patterns behind an inclined flat plate. They found that the strength of the vortices shed from the leading edge and the trailing edges is unequal. Additionally, the wake instabilities were observed to depend on the angle of attack rather than the Reynolds number. Although several studies on this topic are available, a detailed comparative study to understand the aerodynamic characteristics (e.g. pressure coefficient, vortex shedding mechanisms and wake profiles) is still limited. This is needed to improve the performance of an airfoil.

In order to increase the efficiency of an aircraft, one may redesign the flight characteristic as the movement of flying animals, which has much better flight performance than that of an aircraft. In general, the unsteady nature of the flapping-wing mechanism is responsible for the force production (Dickinson *et al.*, 1999). It thus helps flying animals operate their flight efficiently. Many studies on the wing aerodynamics reveal that a flapping motion of an aerofoil trailing edge can be used to mimic the movement of flying animals (Shyy *et al.*, 2013). To design an efficient aircraft wing, it is of significance to investigate the effects of the trailing-edge flap, especially when the flap is in a dynamic motion. This can alter the wake vortices and the trailing-edge noise. The study of an airfoil with a stationary trailing-edge flap revealed that a noise level can be decreased significantly (Schlanderer, 2017), while the lift production is enhanced up to 26% compared to that without a trailing-edge flap (Li *et al.*, 2014). However, there is a lack of the study of the effects of a moving trailing-edge flap.

In this work, a flapping flight of an aircraft is simplified as a two-link rigid plate. In general, a flat plate with a stationary and moving trailing-edge flap can generate different mechanisms of the unsteady vortex shedding and the sound noise, which would alter the lift and drag. The main aim of this work is to use high-fidelity numerical simulation to explore how the trailing-edge flap influences the aerodynamic forces and investigate an interaction between the trailing-edge vortex and the sound noise.

NUMERICAL APPROACH

The problem considered is compressible flow past an inclined flat plate with a stationary and moving trailing-edge flap, as displayed in figure 1. The non-dimensional form of the conservation equations in a Cartesian coordinate system x_i can be expressed as

mass:

$$\frac{\partial \rho}{\partial t} + \frac{\partial}{\partial x_k}(\rho u_k) = 0, \tag{1}$$

momentum:

$$\frac{\partial}{\partial t}(\rho u_i)+\frac{\partial}{\partial x_k}(\rho u_i u_k)=-\frac{\partial p}{\partial x_i}+\frac{\partial \tau_{ik}}{\partial x_k}, \qquad (2)$$

total energy:

$$\frac{\partial}{\partial t}(\rho E)+\frac{\partial}{\partial x_k}(\rho u_k E)=\frac{\partial}{\partial x_k}\left[u_i\tau_{ik}-u_k p-q_k\right], \qquad (3)$$

where t denotes time, ρ is the fluid density, p is the pressure and u_i is the velocity vector. The total energy E is defined from the temperature T as

$$E=\frac{T}{\left[\gamma(\gamma-1)M^2\right]}+\frac{1}{2}u_i u_i, \qquad (4)$$

while the stress tensor τ_{ik} and heat-flux q_k are given as

$$\tau_{ik}=\frac{\mu}{Re}\left(\frac{\partial u_i}{\partial x_k}+\frac{\partial u_k}{\partial x_i}-\frac{2}{3}\frac{\partial u_k}{\partial x_k}\delta_{ik}\right), \qquad (5)$$

$$q_k=\frac{-\mu}{(\gamma-1)M^2 PrRe}\frac{\partial T}{\partial x_k}. \qquad (6)$$

The freestream Mach number is $M=0.4$, while the Reynolds number Re is set to 1000 and is defined from the freestream velocity U_0 and the chord of the plate L. The Prantdl number and the ratio of the specific heat are set to be constant at $Pr=0.72$ and $\gamma=1.4$. The molecular viscosity μ is computed using Sutherland's law with the Sutherland constant of 0.3686. The system of equations is closed by solving the nondimensional equation of state to obtain the pressure as

$$p=\frac{\rho T}{\gamma M^2}. \qquad (7)$$

The computations are performed via an in-house compressible DNS code, HiPSTAR. The flow solver employs a standard 4th-order central finite-difference scheme with a boundary treatment of Carpenter *et al.* (1999) to discretise all the spatial derivatives in the streamwise (x) and wall-normal (y) directions, while a Fourier method is used in the spanwise (z) direction. Temporal advancement is obtained by an ultra-low-storage five-step 4th-order Runge–Kutta scheme (Kennedy *et al.*, 2000). To enhance the stability of the code, a skew-symmetric splitting scheme of the convective terms and an 11-point shock-capturing filtering of Bogey *et al.* (2009) are used. The code has been validated with various benchmark cases. More details of the code can be seen in, e.g., Sandberg (2015). To represent the inclined plate flat hinged with the trailing-edge flap, a second-order boundary data immersion method (BDIM) (Schlanderer *et al.*, 2017) is employed. The computational domain is $-20\le x/L\le 30.21$, $-15\le y/L\le 15$ and $0\le z/L\le 2\pi$, with a grid resolution of 715×545 points in the x- and y-directions and 48 Fourier modes in the z-direction. A uniform velocity is prescribed at the inflow using an integrated characteristic boundary condition. A zonal characteristic boundary condition (CBC) is employed at the outflow (for $x/L\ge 20$ with 30 points). A CBC is applied at the top and bottom of the computational domain.

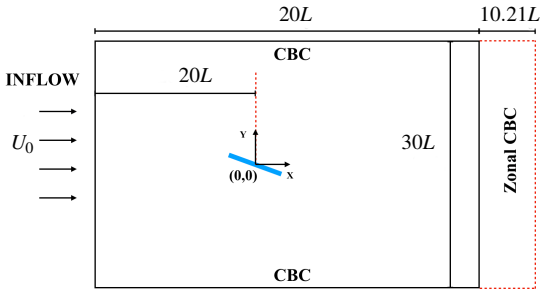

Figure 1. Schematic and coordinate system of flow over an inclined plate.

The plate thickness is set to $0.02L$ with sharp leading and trailing edges, while its angle of attack is $\alpha=20^\circ$. The leading-edge (LE) plate has length $0.75L$ and is stationary, while the trailing edge (TE) moves according to a time-dependent equation. The flapping motion is defined via the angular velocity as $\Omega(t)=\beta\cos(2\pi ft)$ (where β is the amplitude and the frequency f is set to 0.1). Two cases with different amplitude of the angular velocity is investigated, namely (1) stationary trailing-edge flap ($\beta=0$) and (2) moving trailing-edge flap with $\beta=0.33$.

Table 1. Comparison of integral quantities of flow past an inclined plate with different motions of trailing-edge flap.

Cases	Re	$\overline{C}_D$	$\overline{C}_L$	St
2D Stationary TE	1000	0.472	1.021	0.507
2D Flapping TE	1000	0.376	0.898	0.100
3D Stationary TE	1000	0.430	0.946	0.527
3D Flapping TE	1000	0.353	0.837	0.100
2D DNS of Yang *et al.* (2012)	1000	0.3188	1.0381	0.4883
3D DNS of Yang *et al.* (2012)	1000	0.2880	0.9576	0.4959
3D LES of Breuer & Jovičić (2001)	20000	0.38	1.12	0.66

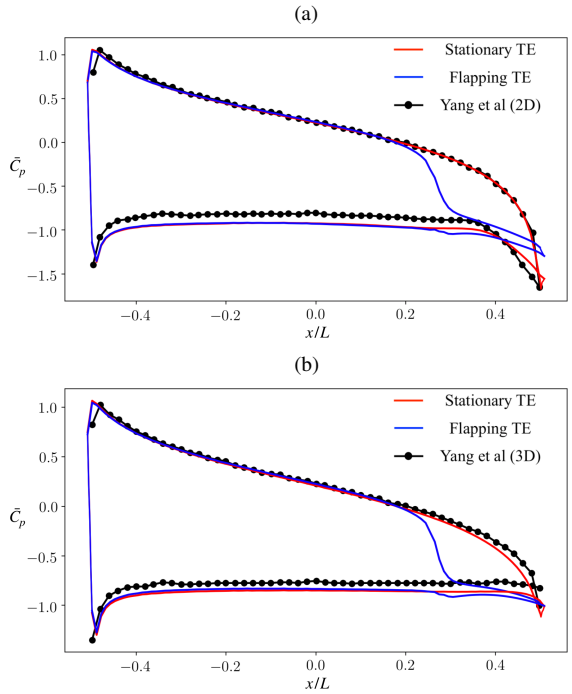

Figure 2. Distribution of time-averaged pressure coefficient $\overline{C}_p$ along the plate surface obtained from (a) two-dimensional and (b) three-dimensional simulations.

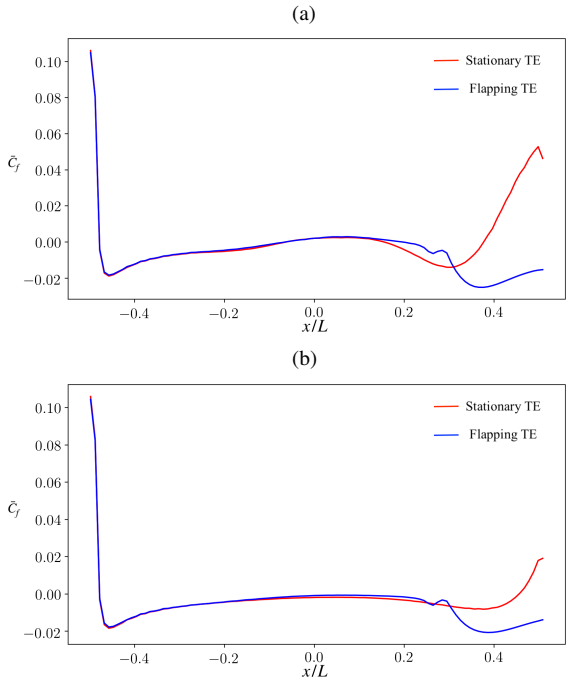

Figure 3. Distribution of time-averaged skin-friction coefficient $\overline{C}_f$ on suction side of the plate obtained from (a) two-dimensional and (b) three-dimensional simulations.

RESULTS

Time-Averaged Flow Fields

The integral quantities obtained from the two-dimensional (2D) and three-dimensional (3D) simulations of the present study are first compared with the published incompressible simulations of Yang *et al.* (2012) and Breuer & Jovičić (2001) to verify the accuracy of the calculation of the aerodynamic forces of the stationary trailing edge cases. The numerical values of the time-averaged drag coefficients $\overline{C}_D$, lift coefficients $\overline{C}_L$, and the Strouhal number $St = fL/U_0$ are given in table 1 (where f is the shedding frequency). It can be seen that $\overline{C}_D$, $\overline{C}_L$ and St of the 2D and 3D stationary TE cases exhibit some minor discrepancies with the data from the literatures due to the compressibility effects. Once the trailing edge flaps, the Strouhal number reduces to the flapping frequency of $St = 0.1$, while the values of $\overline{C}_D$ and $\overline{C}_L$ decrease.

The distribution of the time-averaged pressure coefficient $\overline{C}_p = 2(\bar{p} - p_0)/\rho U_0^2$ for 2D and 3D simulations is given in figure 2. The incompressible results of Yang *et al.* (2012) are also plotted for comparison. For the stationary TE cases, the profile of $\overline{C}_p$ on the pressure side matches well with that of Yang *et al.* (2012). Although $\overline{C}_p$ on the suction side of this case is similar to that of Yang *et al.* (2012), its magnitude is slightly lower. This happens because the difference in the structure of the separation bubble, which is altered by the sound pressure. The moving motion of the trailing-edge flap does not have much influence on $\overline{C}_p$ on the suction side. In contrast, the distribution of $\overline{C}_p$ on the pressure side changes dramatically after $x/L \approx 0.2$. The profile of the time-averaged skin-friction coefficient $\overline{C}_f = 2\overline{\tau}_w/\rho U_0^2$ suggests that the flow on most of the suction side is separated, as display in figure 3. The flapping motion of the rear part of the plate alters the separated shear layer near the trailing edge. This leads to the modification of the formation of the leading-edge and trailing-edge vortices.

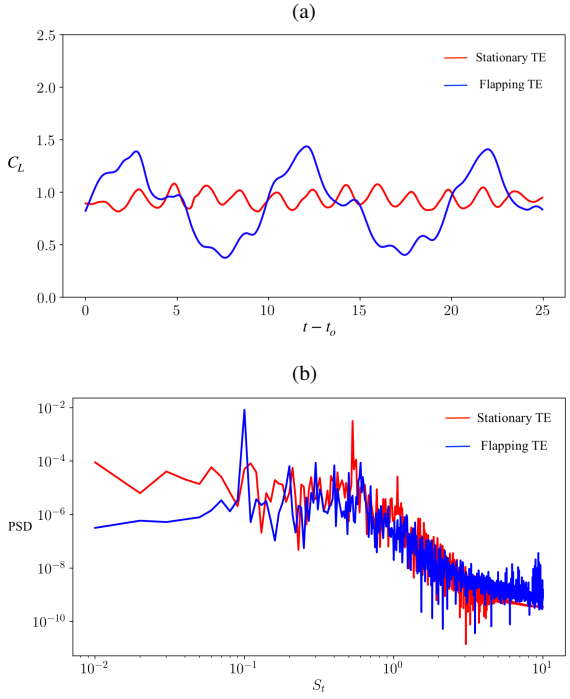

Figure 4. (a) Histories of the lift coefficient of the 3D simulation. (b) Power spectral density (PSD) of the lift coefficient.

Vortical Structures

This section investigates the effect of the flapping trailing edge on the formation of the vortex shedding and the acoustic field. Only the results from the 3D simulations are presented. To quantify the relationship between the generation mechanism of the of the lift and the vortex shedding process, histories of C_L together with its power spectral density (PSD) are illustrated in figure 4. Different dominant

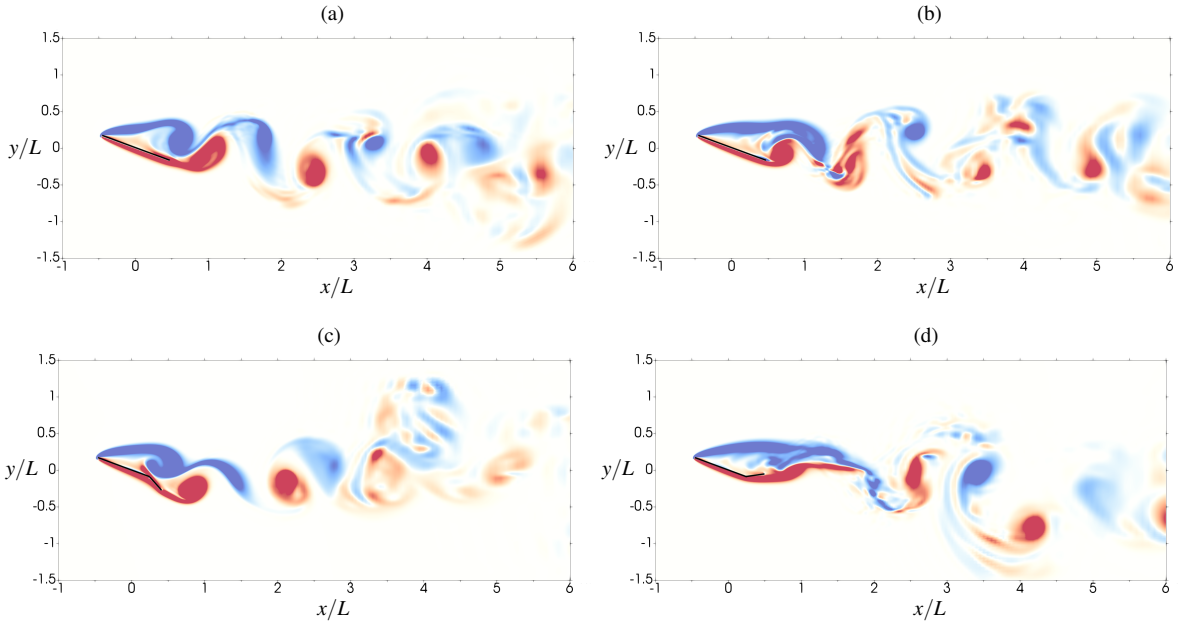

Figure 5. Contours of instantaneous spanwise vorticity ω_z in the midspan plane of flow over an inclined plate with (top panel) stationary and (bottom panel) moving trailing-edge flap at the time when C_L reaches (a,c) the maximum and (b, d) the minimum values. Vorticity varies from $-5 \leq \omega_z \leq 5$. Blue and red patches respectively show negative and positive vorticity.

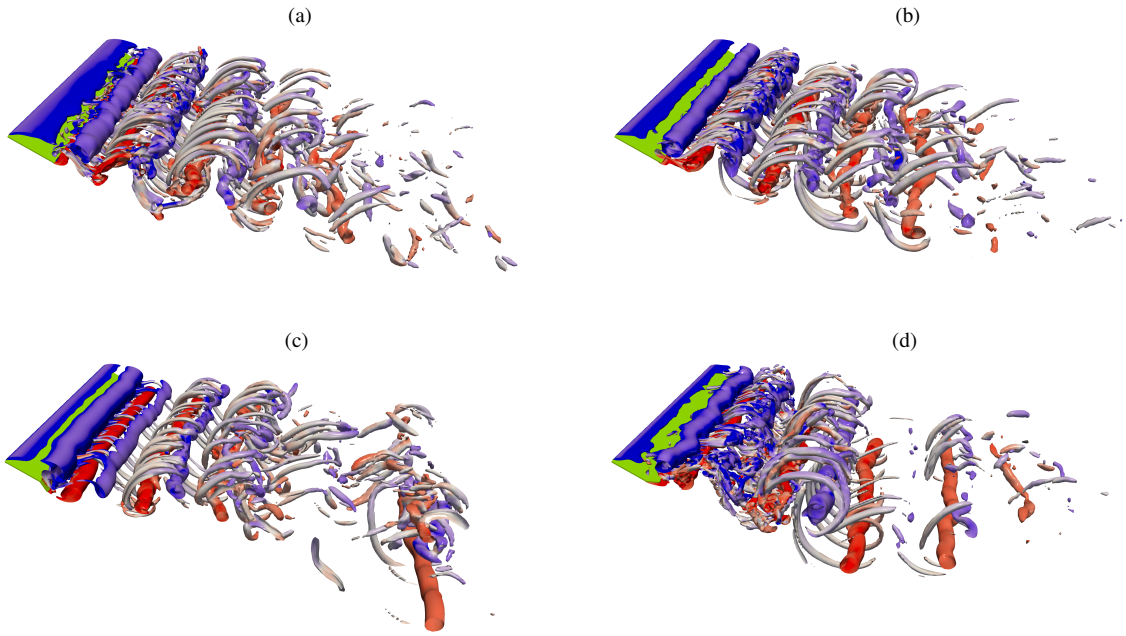

Figure 6. Instantaneous coherent structures, visualised by the isosurfaces of Q, of flow over an inclined plate with (top panels) stationary and (bottom panels) moving trailing-edge flap at the time when C_L reaches (a,c) the maximum and (b, d) the minimum values.

shedding frequencies of the flow are clearly observed when the trailing-edge flap is in different motions (figure 4a). In addition, the magnitude of C_L of the flapping TE case is higher. The PSD of C_L displayed in figure 4(b) shows that the most dominant shedding frequency for the stationary TE case is $St = 0.527$ and is reduced to $St = 0.1$ when the trailing edge flaps (see also table 1).

The contours of the instantaneous spanwise vorticity ω_z at the time when the C_L reaches the maximum and minimum values are given in figure 5. For both cases, the asymmetric vortex street periodically sheds behind the plate, but with different shedding formations. When the tailing-edge flap is stationary, the primary vortices occur alternatively at the leading edge and the trailing edge. The vortices then form a regular vortex street in the wake, as illustrated in figures 5(a) and 5(b). Since the dynamic motion of the trailing-edge flap alters the formation of the leading-edge and trailing-edge vortices, the vortex shedding process in one shedding period of this case consists of different formations of the vortex pair (see figures 5c and 5d). The relationship between the vortex shedding process and the generation mechanism of C_L can be explained as follows. The inclined plate generates the maximum lift during the shedding of the trailing-edge vortex (figures 5a and 5c). The

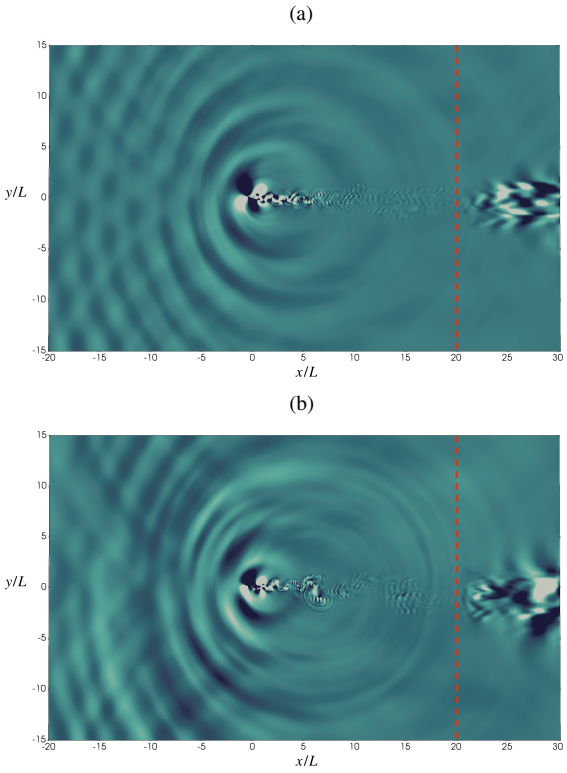

Figure 7. Contours of dilatation $\boldsymbol{\nabla \cdot u}$ of flow over an inclined plate with (a) stationary trailing-edge flap and (b) moving trailing-edge flap. Dilatation varies from $-0.01 \leq \boldsymbol{\nabla \cdot u} \leq 0.01$. The dashed line denotes onset of the zonal CBC.

minimum C_L occurs once the trailing-edge vortex is still attached to the plate, as displayed in figures 5(b) and 5(d).

Instantaneous flow structures at maximum and minimum C_L are also visualised by means of the second invariant of the velocity gradient tensor $Q = -0.5 u_{i,j} u_{j,i}$ (for details see Jeong & Hussain, 1995), as shown in figure 6. The evolution of the coherent structures is relevant to the spanwise vortices. It can be observed that the spanwise vortex rollers are shed nearly parallel to the plate. The shear layers then break up into small-scale turbulence immediately behind the leading-edge and trailing-edge vortices. The effects of the trailing-edge flap on the formation of the vortex street at the maximum and minimum C_L are clearly seen. In addition, the leading-edge vortex seems to be distorted along the spanwise direction by the flapping motion of the trailing edge when the plate is under the minimum lift. This results in the rapid breakdown to turbulence and more irregular vortical structures in the near-wake region.

Figure 7 displays contour plots of the dilatation $u_{i,i}$ in order to investigate the resulting acoustic field. It can be seen that the noise originates from the front part of the plate with the strongest noise level in the upstream direction and on the suction side, presumably due to the interaction of the wall and the pressure fluctuations from the flow separation and the associated vortex shedding. The noise then radiates away from the plate with different patterns and frequencies, depending on the characteristics of the trailing-edge motion. The noise pattern of the flapping TE case is less organised compared to that of the stationary TE case. It is worth noting that no signs of spurious pressure reflections from any other boundary of the computational domain into the region of interest are observed.

SUMMARY

Numerical simulations of unsteady compressible flow around an inclined flat plate with a stationary and moving trailing-edge flap have been performed using DNS. The numerical results show that different motions of the trailing-edge flap can remarkably influence the formation of the leading-edge and trailing-edge vortices. It thus modifies the resulting separation bubble. This leads to the change in the structures of the vortex shedding and the associated acoustic noise, which eventually alters the aerodynamic forces.

ACKNOWLEDGMENTS

This work is supported by the Thailand Research Fund (TRF). NB and JT would like to acknowledge the scholarships from the Graduate School and the Faculty of Engineering, Chiang Mai University. The computational resources provided by the National e-Science Infrastructure Consortium are highly appreciated.

REFERENCES

Bogey, C., de Cacqueray, N. & Bailly, C. 2009 A shock-capturing methodology based on adaptative spatial filtering for high-order non-linear computations. *J. Comput. Phys.* **228** (5), 1447–1465.

Breuer, M. & Jovičić, N. 2001 Separated flow around a flat plate at high incidence: An LES investigation. *J. Turbul.* **2** (N18), 1–15.

Carpenter, M. H., Nordström, J. & Gottlieb, D. 1999 A stable and conservative interface treatment of arbitrary spatial accuracy. *J. Comput. Phys.* **148** (2), 341–365.

Dickinson, M. H., Lehmann, F.O. & P., Sane. S. 1999 Wing rotation and the aerodynamic basis of insect flight. *Science* **284** (5422), 1954–1960.

Jeong, J. & Hussain, F. 1995 On the identification of a vortex. *J. Fluid Mech.* **285**, 69–94.

Kennedy, C. A., Carpenter, M. H. & Lewis, R. M. 2000 Low-storage, explicit Runge–Kutta schemes for the compressible Navier–Stokes equations. *Appl. Numer. Math.* **35** (3), 177–219.

Lam, K. M. & Wei, C. T. 2010 Numerical simulation of vortex shedding from an inclined flat plate. *Eng. Appl. Comp. Fluid Mech.* **4** (4), 569–579.

Li, C., Dong, H. & Ren, Y. 2014 A numerical study of flapping plates hinged with a trailing-edge flap. *AIAA Paper 2014-2049*.

Sandberg, R. D. 2015 Compressible-flow DNS with application to airfoil noise. *Flow Turbul. Combust.* **95** (2–3), 211–229.

Schlanderer, S. C. 2017 A virtual boundary method for compressible flow with application to aeroacoustics of compliant trailing-edges. PhD thesis, University of Southampton, Southampton, UK.

Schlanderer, S. C., Weymouth, G. D. & Sandberg, R. D. 2017 The boundary data immersion method for compressible flows with application to aeroacoustics. *J. Comput. Phys.* **333**, 440–461.

Shyy, W., Aono, H., Kang, C.-K. & Liu, H. 2013 *An Introduction to Flapping Wing Aerodynamics*. New York, NY: Cambridge University Press.

Yang, D., Pettersen, B., Andersson, H. I. & Narasimhamurthy, V. D. 2012 Vortex shedding in flow past an inclined flat plate at high incidence. *Phys. Fluids* **24** (8), 084103.